arXiv:1610.05916v1 [cond-mat.soft] 19 Oct 2016

Estimation of the critical behavior in an active colloidal system with Vicsek-like interactions

Benjamin Trefz,[1,2] Jonathan Tammo Siebert,[1] Thomas Speck,[1] Kurt Binder,[1] and Peter Virnau[1]
[1)] *Johannes Gutenberg University Mainz, Department of Physics, Staudingerweg 7, 55128 Mainz, Germany*
[2)] *Graduate School Material Science in Mainz, Staudinger Weg 9, 55128 Mainz, Germany*

(Dated: October 20, 2016)

We study numerically the critical behavior of a modified, active Asakura-Oosawa model for colloid-polymer mixtures. The colloids are modeled as self-propelled particles with Vicsek-like interactions. This system undergoes phase separation between a colloid-rich and a polymer-rich phase, whereby the phase diagram depends on the strength of the Vicsek-like interactions. Employing a subsystem-block-density distribution analysis, we determine the critical point and make an attempt to estimate the critical exponents. In contrast to the passive model, we find that the critical point is not located on the rectilinear diameter. A first estimate of the critical exponents β and ν is consistent with the underlying 3d-Ising universality class observed for the passive model.

Keywords: Active particles ; non-equilibrium ; critical point ; Vicsek ; Asakura-Oosawa model

I. INTRODUCTION

Active particles are intrinsically non-equilibrium systems which have some means of self-propulsion. This can be a motor or flagellum, but can also be induced by the solvent and/or external sources. In all cases, some form of energy is converted into kinetic energy that results in the self-propulsion. This general definition encompasses a large variety of systems on different scales. Besides rather large macroscopic systems such as flock of birds or school of fish[1,2], active particles are also found on a micrometer scale. Such systems include actin filaments[3], and microtubules[4,5] that are moved by motor proteins in a plane and can be observed via microscopes. Some bacteria are able to propel themselves and can show density-dependent phase separation[6,7]. Sperm cells cooperate due to hydrodynamic interactions and form clusters[8]. It is even possible to alter microorganisms and make them thereby active, e.g. by attaching an artificial, magnetically activated flagellum[9]. Another approach is to combine an already self-propelled particle, e.g. a sperm cell, with an externally controllable non-motile part, e.g. a magnetic microtube[10].

In soft matter systems, colloids play an important role as a model system since they provide an ideal environment to compare experiment, computer simulation, and theory. In particular, interactions between colloidal particles are tunable, and one can follow the motion of individual colloids by confocal video microscopy techniques. Active particles are no exception and a variety of systems with self-propelled particles have been studied. Colloidal systems that are driven from the outside allow for direct comparison of the active and the passive system. Self-propulsion can be achieved in many ways, e.g. thermophoresis, diffusiophoresis, or electrophoresis. Thermophoresis can be realized via an external light source that heats the sample generating a temperature gradient[11]. Self-diffusiophoresis has been observed in a binary, near-critical solvent[12]. Other swimmers exploit a chemical reaction to maintain a local gradient[13–16]. In these examples, the solution contains hydrogen peroxide and the active constituents are so-called Janus-type particles, where one hemisphere is coated with platinum. The conducting hemisphere acts as catalyst for the reaction of hydrogen peroxide to water and oxygen and thus "consumes" the fuel, which in turn propels the particle forward. Self-propulsion induced by electric fields can be realized via Quincke rotation of the colloid[17] or via a metallic Janus-type particles[18].

In the last years several different models to study active particles have been discussed[19–25]. Many active systems show the tendency to form clusters, e.g., flock of birds, school of fish, and colony of bacteria. This raises the question of phase separation, which has been analyzed in various numerical investigations[22,23,25–29]. Studies with active particles often consist of active and passive particles, e.g., motile bacteria in a polymer background[30–32]. The model we study here is a variation of the well known Asakura-Oosawa (AO) model[33–38], which consists of two particle types, colloids and polymers. In our active model, the colloidal particles become self-propelled with Vicsek-like interactions[22,25]. This facilitates the phase separation compared to the passive model, since the Vicsek-like activity induces the formation of clusters. This result, together with the static and dynamic behavior of this model, has been reported in[22,25]. Importantly, the passive AO model already features a phase transition and belongs to the Ising universality class. From the active model, the passive model is recovered in the limit when the strength of the self-propulsion goes to zero.

A very interesting question is whether critical phenomena in a non-equilibrium system belong to a known universality class of some related equilibrium system or form a new class. A first step to address this issue, of course, is to find the location of the critical point. For systems under shear[39] one finds that the system changes its behavior towards the mean-field universality class in the limit of infinite shear[40]. The critical point of the classical Vicsek

model has been determined successfully[41,42]. It should be noted that this was a heavily discussed issue, and the continuous phase transition from disordered to ordered state was questioned[43]. It was later shown that the way noise is introduced in the classical Vicsek model can change the order of the phase transition[44,45]. For the determination of the critical point numerous simulations at different system sizes, densities and noise values had to be performed. A different approach has recently been proposed[46], where the critical point of an active Lennard-Jones system has been determined by fitting various power laws and assuming an exponential dependence on parameters. In other models, the critical point in the active case turned out to be at infinite density and could thus not be determined directly via simulation[47].

In this paper, we will discuss the determination of the critical point in a system of self-propelled particles using the subsystem-block-distribution analysis. The method will be general and thus should apply to any density-driven phase separation that features a second order phase transition. Exemplary we will determine the critical point of our active Asakura-Oosawa model.

II. MODEL AND METHODS

Let us first recall why the location of the critical point of a non-equilibrium system is much more difficult to find than for an equilibrium system. In the latter, we can study the phase behavior choosing an intensive thermodynamic variable as a control variable; e.g. in a colloid-polymer mixture the chemical potential of the polymers (or a related variable, such as the so-called polymer reservoir packing fraction η_p^r) are commonly used. In the resulting phase diagram, the critical point then occurs at the minimum of the coexistence curve, and the tie lines connecting coexisting vapor-like and liquid-like phases of the colloidal suspension are horizontal lines (Figure 1(a)). In thermal equilibrium, the thermodynamic relations allow the translation of this phase diagram in a representation with two densities of extensive variables, the colloid packing fraction $\eta_{\rm col}$ and the polymer packing fraction $\eta_{\rm pol}$ (Figure 1(b)). Then the tie lines no longer are horizontal lines but rather are oriented under an a priori unknown angle, and the critical point is not on a straightforwardly defined position on the coexistence curve, but rather nontrivial to find in this statistical ensemble.

In the non-equilibrium system containing active colloids, intensive thermodynamic variables no longer are well-defined, in contrast to extensive variables (number of colloids $N_{\rm col}$ and number of polymers $N_{\rm pol}$ in the considered volume) and their densities, which are still well defined. We ask whether phase separation in a gas-like and liquid-like phase also occurs, and if so, estimate the corresponding phase diagram. This task was already attempted in Refs. 22,25, looking for phase coexistence in simulation volumes elongated in z-direction, where in the two phase region a liquid domain separated by two

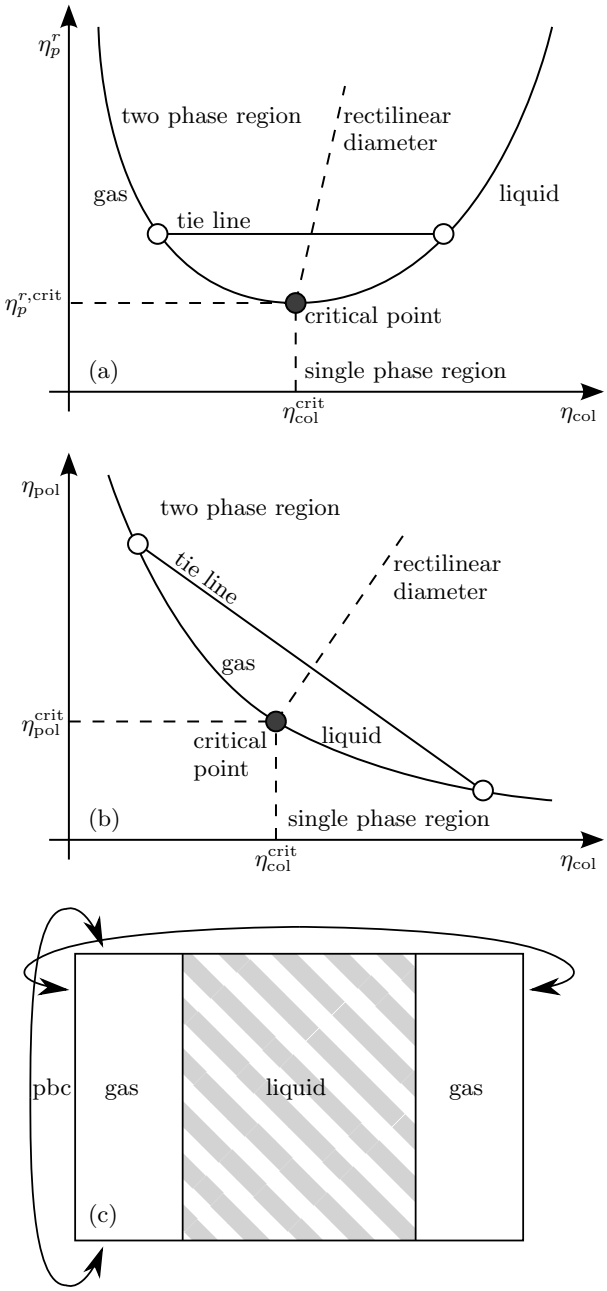

Figure 1. Schematic drawing of (a) the phase diagram for the colloid packing fraction $\eta_{\rm col}$ plotted against the intensive thermodynamic variable η_p^r, (b) the phase diagram for two extensive variables $\eta_{\rm col}$ and $\eta_{\rm pol}$. (c) shows a schematic representation of a system in the two phase region. The two tie points from (b) can be obtained by extracting the packing fractions in the liquid and the gas phases. With this recipe the coexistence curve in Figure 2 has been determined.

(on average planar) interfaces from the gas occurs (Figure 1(c)). This means that the local densities of colloids and polymers separate in gas and liquid domains, and the end points of the tie line in Figure 1(b) can be found, but only for states far away from the critical point. For finding the location of the critical point, obviously a

different approach must be sought, since near criticality the density differences between the coexisting phases are small. Strong and long-lived density fluctuations occur, and the interfaces become very rough and diffuse. The same difficulty would occur if we would use $\eta_{\rm col}$, $\eta_{\rm pol}$ as variables in a simulation of a colloid-polymer mixture in equilibrium, but there Figure 1(a) provides for a more convenient alternative, e.g. one records the probability distribution $P(\eta_{\rm col})$ at fixed η_p^r, finding the end-points of the tie line in Figure 1(a) from the peaks of that distribution, and analyzing the merging of the peaks near criticality in terms of a finite size scaling analysis[36].

In the following, we study a model of Vicsek-like interactions between active particles. A detailed description of the model can be found in Refs. 22,25. The binary system is a variant of the well-known Asakura-Oosawa (AO) model and consists of colloids (c) and polymers (p)[37]. The potentials are given by:

$$U_{cc}(r) = 4\epsilon_{cc}\left[\left(\frac{\sigma_{cc}}{r}\right)^{12} - \left(\frac{\sigma_{cc}}{r}\right)^{6} + \frac{1}{4}\right] \quad (1)$$

$$U_{cp}(r) = 4\epsilon_{cp}\left[\left(\frac{\sigma_{cp}}{r}\right)^{12} - \left(\frac{\sigma_{cp}}{r}\right)^{6} + \frac{1}{4}\right] \quad (2)$$

$$U_{pp}(r) = 8\epsilon_{pp}\left[1 - 10\left(\frac{r}{r_{pp}}\right)^{3} + 15\left(\frac{r}{r_{pp}}\right)^{4} - 6\left(\frac{r}{r_{pp}}\right)^{5}\right] \quad , \quad (3)$$

if r is smaller than the respective cut-off radius $r_{cc} = 2^{1/6}\sigma_{cc}$, $r_{cp} = 2^{1/6}\sigma_{cp}$, $r_{pp} = 2^{1/6}\sigma_{pp}$, and zero otherwise. The other parameters are chosen according to[22,25,37] $\epsilon_{cc} = \epsilon_{cp} = 1$, $\epsilon_{pp} = 0.0625$, $\sigma_{cc} = 1$, $\sigma_{cp} = 0.9$, and $\sigma_{pp} = 0.8$. To be consistent with the literature, we calculate the packing fractions η_α as $\eta_\alpha = \rho_\alpha V_\alpha$, where $V_\alpha = \pi d_\alpha^3/6$ is the volume of a single sphere and d_α is the Barker-Henderson diameter[48] of the colloids or in case of the polymers $0.8 d_{cc}$. To thermostat the system we use a Langevin thermostat in our MD simulation[49,50].

The equations of motion are

$$m\ddot{\vec{r}}_i = -\vec{\nabla}U - \gamma m\dot{\vec{r}}_i + \sqrt{2\gamma k_B T m}\,\vec{R}_i(t) \quad , \quad (4)$$

where $m = 1$ is the particle mass (for all particle types), $\gamma = 1$ is the friction coefficient, U is the interparticle potential, $T = 1$ is the temperature, and $\vec{R}$ is a zero-mean unit-variance Gaussian white noise. We use a Velocity Verlet algorithm with a time step $\Delta t = 0.002 t_0$, with $t_0 = \sqrt{\sigma_{cc}^2 m/\epsilon_{cc}}$.

In the active version we employ a variation of the Vicsek model[22,25] on top of the passive AO model for the colloids. For that we still solve the Langevin equation first just as in the passive model. The resulting velocity is then modified by an additional force

$$\vec{f}_i = f_A \cdot \frac{\langle \vec{v}_j \rangle_R}{\langle |\vec{v}_j| \rangle_R} \quad (5)$$

acting on particle i. The constant force is set to $f_A = 0$ for the polymers and $f_A = 10$ for the colloids in this work. The brackets $<>_R$ denote an average over all colloids in a sphere of radius R, with $R = \sqrt{2}\, r_{cc}$ being the cut-off radius for what is considered a neighbor. In the active model we observe enhanced phase separation, as can be seen in Figure 2, and which was already discussed in Refs. 22,25.

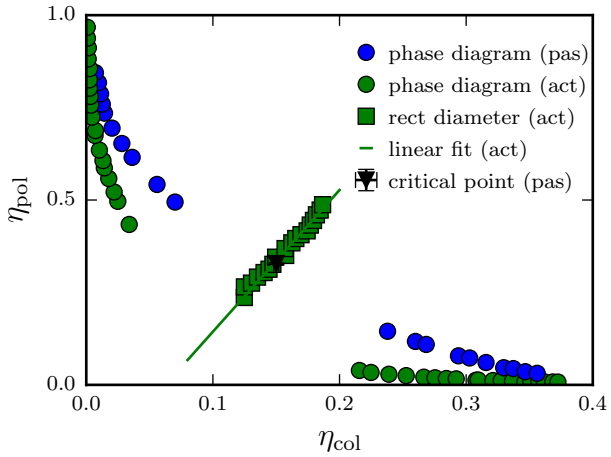

Figure 2. Phase diagram of the active and passive system together with a fit of the rectilinear diameter of the active system (Eq. (9)). The critical point of the passive system is taken from[37].

This system is out of equilibrium, and the temperature T used in Eq. (4) does not characterize fluctuations of velocity or other variables in the system as demonstrated in earlier work[22,25]. As discussed in the introduction, the distribution function $P(\eta_{\rm col}, \eta_{\rm pol})$ is the quantity that contains the desired information on phase separation (and associated criticality) in the system. However, in our system (we choose a cubic box of linear dimension S with periodic boundary conditions throughout, containing $N_{\rm col}$ colloids and $N_{\rm pol}$ polymers) both $\eta_{\rm col}$ and $\eta_{\rm pol}$ are fixed, and hence the distribution function of the total system is meaningless. However, a way out of this dilemma is the application of the so-called subsystem-block-density distribution[51–54] which we will refer to as subbox method. Here, a big canonical simulation box is simulated and divided into many smaller subboxes. In these subboxes the particle number is allowed to fluctuate, thus a "quasi" grand canonical system is simulated. For each subbox we can then determine the higher moments of the density distribution

$$m^2(\alpha) = \frac{1}{N^3}\sum_i \left(\rho_i(\alpha) - \bar{\rho}(\alpha)\right)^2 \quad (6)$$

$$m^4(\alpha) = \frac{1}{N^3}\sum_i \left(\rho_i(\alpha) - \bar{\rho}(\alpha)\right)^4 \quad (7)$$

and calculate the cumulant as

$$U_N(\eta_\alpha) = \frac{\langle m(\alpha)^4 \rangle}{\langle m(\alpha)^2 \rangle^2} \quad , \quad (8)$$

where α is either col or pol, $\rho_i(\alpha)$ is the density of particle α in subbox i, $\bar{\rho}(\alpha)$ is the average density of particles of type α in the system, and N^3 is the total number of subboxes of the system. Note that in Eq. (8) the average $\langle ... \rangle$ indicates an average over multiple, independent simulation snapshots, while m^2 and m^4 are already averaged over all subboxes of the same size. With this method the same $N_{\mathrm{col}}N_{\mathrm{pol}}$VT trajectory can be used to compute all subbox systems simultaneously. This reduces the computation time substantially, although care is required, since the fluctuations observed for different subbox sizes L clearly are not uncorrelated.

For the analysis one has to select proper subbox sizes. In Ref. 53 the authors estimate that the subbox size L should be chosen in a way that $\xi \ll L \ll S$, where ξ is the correlation length and thus a priori unknown but constant. Unfortunately, there is no obvious way to choose the optimal subbox sizes. Surely, the resulting subbox volume should not be too small, since the fluctuation of the density, corresponding to the addition or subtraction of a single particle, is getting bigger. Hence, the studied distribution would change from Gaussian to Poissonian. On the other hand the subbox should not be too big, as then there are too few subboxes and the correlation between them is increasing. Therefore, the overall explored phase space gets to narrow and thus the systematic errors due to the finite size of S become too large (the finite size analysis[51–53] ignores the presence of a further non-zero scaling variable L/S completely!). Since both effects are difficult to quantify, we choose the subbox sizes empirically, by only using subboxes that show a reasonable behavior far from the critical point.

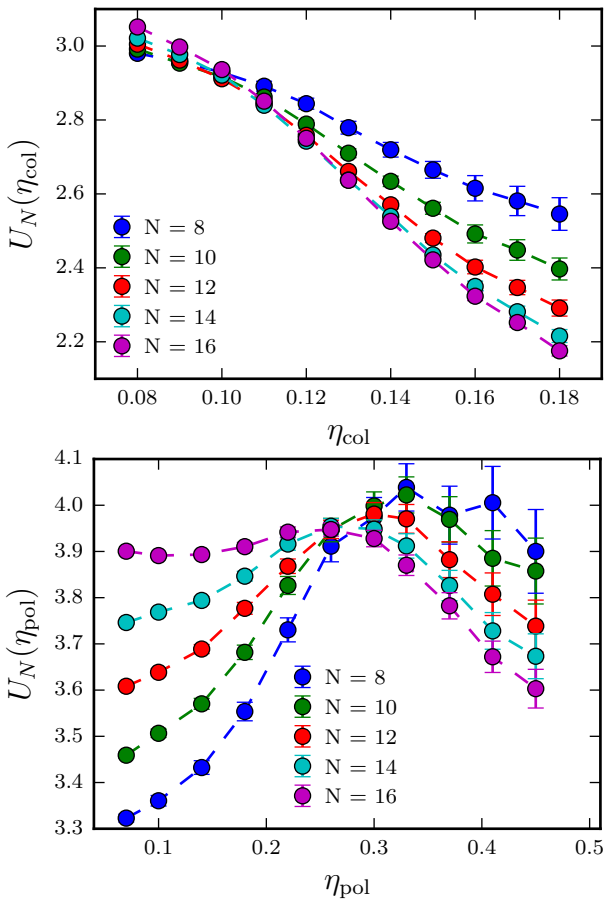

Figure 3. Crossing of the Binder cumulants along state points on the fitted rectilinear diameter from Figure 2. (a) The colloid cumulant $U_N(\eta_{\mathrm{col}})$ is plotted against the colloid packing fraction η_{col}. The intersection point is read off as $\eta_{\mathrm{col}}^{\mathrm{crit}} = 0.103(5)$. (b) The same state points are analysed for the polymers. The intersection is at state points with higher densities than for the colloids, thus the statistical error of this intersection is larger. The critical polymer packing fraction is estimated as $\eta_{\mathrm{pol}}^{\mathrm{crit}} = 0.278(8)$.

III. RESULTS

A. Rectilinear diameter

In order to determine the critical point of the active ($f_A = 10$) system we use an iterative approach. First we assume that the law of rectilinear diameter, which the passive system approximately follows, is still true in the non-equilibrium model and we can thus write

$$\frac{1}{2} \cdot (\eta_{\mathrm{pol}}^{\mathrm{gas}} + \eta_{\mathrm{pol}}^{\mathrm{liquid}}) = \frac{a}{2} \cdot (\eta_{\mathrm{col}}^{\mathrm{gas}} + \eta_{\mathrm{col}}^{\mathrm{liquid}}) + b \quad . \qquad (9)$$

The rectilinear diameter for the active system is shown in Figure 2 as green squares and the green line represents the fit to Eq. (9), where $a = 3.83$ and $b = -0.24$ are the resulting fit parameters. For the known region of the phase diagram, the active model seems to follow the law of rectilinear diameter and its difference to the passive system is minor, as the critical point of the passive system falls nicely onto the fit. However, it should be remembered that the "law of rectilinear diameter"[55] is not a general law of statistical thermodynamics, but rather can be derived only in the framework of mean field type theories. In fact, very close to the critical point deviations from this "law" are expected already for systems in thermal equilibrium[56–58], but for passive systems deviations are typically negligible. Therefore, we assume for now that the active system also follows the law of rectilinear diameter and simulate the active system for different state points along the green line in Figure 2. We use a cubic simulation box with $S = 48\sigma_{cc}$ and subdivide the system into many small subboxes $N = 8, 10, 12, 14, 16$ to calculate the moments and cumulants as defined in Eqs. (6)-(8). The length of each subbox is then $L = S/N$. In Figure 3, the intersection of the Binder cumulants U_N are shown along the path of the rectilinear diameter. In the ideal case (where the limit $S \to \infty$ could be taken and L is extremely large), one would hope that the cumulants cross in a single (L-independent) crossing point. In reality, this is not the case, the crossing points are spread out over some region (this is expected due to the

fact that L and S are not large enough to reach the finite size scaling limit fully)[53]. However, from the multiple crossings one can use the average value as an estimate for the crossing point and the standard deviation as an estimate of error. For the critical colloid packing fraction we find $\eta_{\text{crit}}^{\text{col}} = 0.103(5)$, while the critical polymer packing fraction is determined as $\eta_{\text{crit}}^{\text{pol}} = 0.278(8)$. While both cumulants $U_N(\eta_{\text{col}})$ and $U_N(\eta_{\text{pol}})$ cross for all sub-box sizes analyzed, the crossing occurs at different state points. Thus, the critical point will not fall onto this line of rectilinear diameter but will be slightly shifted. Note that a deviation from the law of rectilinear diameter has been observed for a different active model as well[46]. In an equilibrium system, it has been shown that the critical parameters can reasonably well be determined independently of each other[53]. Therefore, we can interpret the cumulant intersections as an approximation of the critical point. In the following we will improve the accuracy with which the critical point is estimated by two independent approaches.

B. Extrapolation from the homogeneous region

Due to the rather large value of the slope of the rectilinear diameter the colloid packing fraction has a better accuracy than the polymer packing fraction, which can also be seen in Figure 3. Therefore, we determine the critical polymer packing fraction by extrapolating the susceptibility from the homogeneous phase to the critical colloid packing fraction, which for now we assume to be correct. For that the order parameter susceptibility is determined from the two dimensional probability distribution $P(N_{\text{col}}, N_{\text{pol}})$ which, in the homogeneous phase, has contour lines that are ellipses. As shown in Ref. 37, the susceptibility is proportional to

$$\chi_+ \propto \frac{(\text{HWHM})^2}{N_{\text{col}} + N_{\text{pol}}} = W_+ \quad . \tag{10}$$

Here HWHM stands for the half-width half-maximum of the long axis of $P(N_{\text{col}}, N_{\text{pol}})$, which is determined by fitting an ellipse to the distribution's equi-probability line at $0.5P_{\text{max}}$.

We simulate state points on various paths that cross the rectilinear diameter and determine the maximum of the susceptibilities on each of them. One exemplary path is shown as the black dotted line in Figure 4. The inset of the same figure shows the determined values of W_+ along this line and the region where the order parameter susceptibility reaches a maximum is colored in gray. In order to extrapolate the susceptibility to the critical point, we are only interested in the position of this maximum, not the numerical value which would be needed in order to investigate the scaling behavior. In the thermodynamic limit the susceptibility will diverge at the critical point. Due to finite size effects this can not happen in our simulation, but the susceptibility will

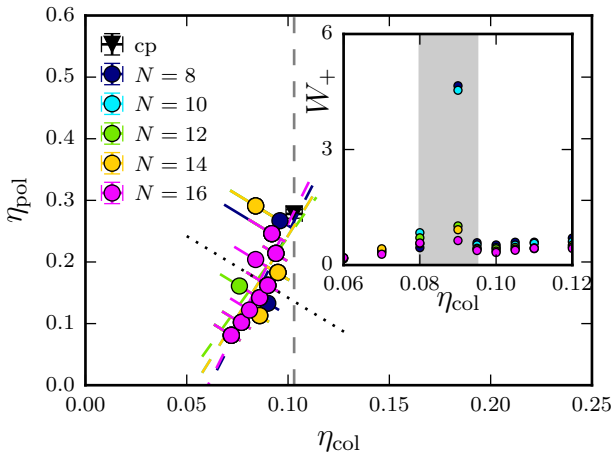

Figure 4. Extrapolation of the maximum order parameter susceptibility χ_+ determined for individual slopes in the phase diagram. The error bars indicate the distance to the next simulated state point, and can thus be asymmetrical. The locus of maximal susceptibility indicates a linear behavior over a long range of state points and can thus be extrapolated to the critical colloid packing fraction $\eta_{\text{col}}^{\text{crit}} = 0.103$ to determine $\eta_{\text{pol}}^{\text{crit}} = 0.264(10)$. The inset shows the value of $W_+(\propto \chi_+)$ along the black dotted line. The used colors correspond to the ones used in the main legend. Note that the height of the maximum can not be extracted from this analysis. However, we are only interested in the position of χ_+, which can be estimated to be inside the gray area of the inset.

reach a maximum nonetheless. Therefore, plotting only the positions of the maximums on each path allows us to extrapolate them towards the critical colloid packing fraction and thus find an approximation for the correct critical polymer packing fraction as shown in Figure 4. The critical polymer packing fraction is determined to be $\eta_{\text{pol}}^{\text{crit}} = 0.264(10)$, which is slightly lower than the value from the simulation along the rectilinear diameter.

C. Cumulant intersection for constant packing fractions

As an alternative, we determine the critical packing fractions by simulating along a line in the parameter space that keeps one packing fraction constant. We use the result obtained in the previous section and simulate along a constant colloid packing fraction of $\eta_{\text{col}} = 0.103$ and a constant polymer packing fraction of $\eta_{\text{pol}} = 0.264$. The simulated state points are shown in Figure 5.

From the intersection of the polymer cumulants at constant colloid packing fraction we determine the critical polymer packing fraction which should be in agreement with the polymer packing fraction that we determined before. The run at constant polymer packing fraction is done to determine that the initial assumption was correct and the critical colloid packing fraction could be ex-

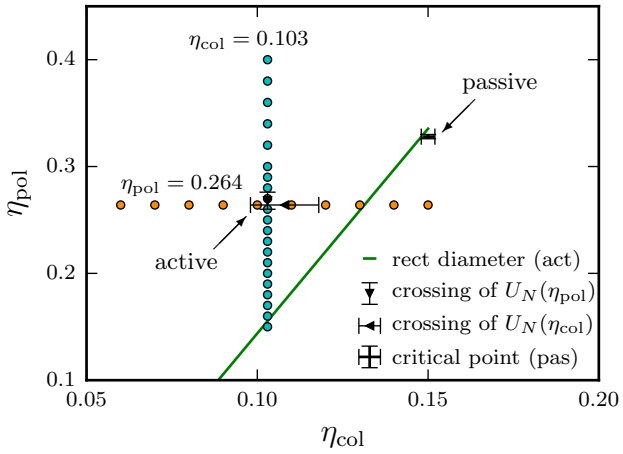

Figure 5. The simulated state points at constant colloid packing fraction (cyan) and constant polymer packing fraction (orange) are shown together with the fitted rectilinear diameter (Figure 2) of the active system and the critical point of the passive system taken from[37]. The intersections of both cumulants (Figure 6) are shown as black triangles. They overlap inside the error bars and clearly deviate from the rectilinear diameter.

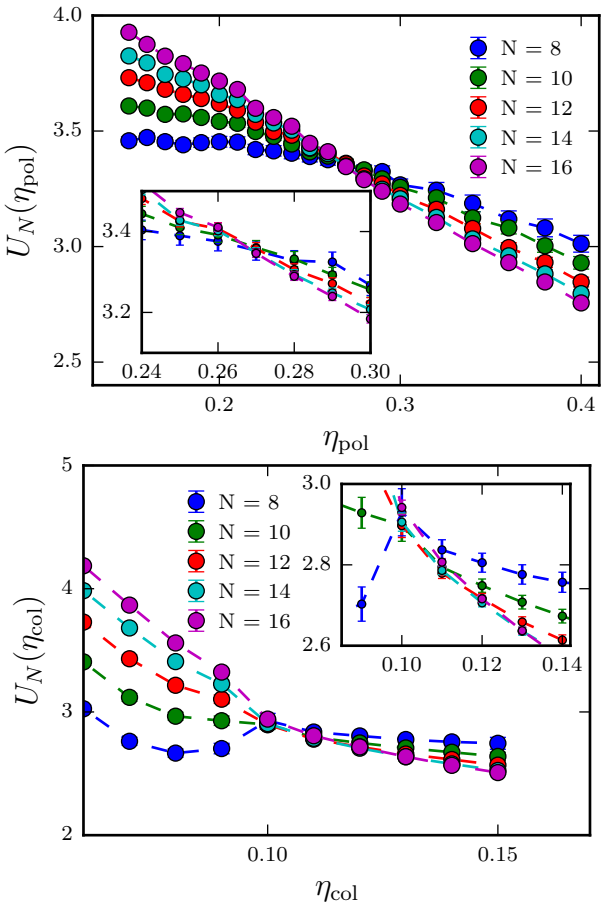

Figure 6. Crossing of the Binder cumulants along state points on a line of constant (a) colloid (b) polymer packing fraction as shown in Figure 5. (a) The polymer cumulant $U_N(\eta_{\rm pol})$ is plotted against the polymer packing fraction $\eta_{\rm pol}$ at constant $\eta_{\rm col}^{\rm crit} = 0.103$. The intersection point is read off as $\eta_{\rm pol}^{\rm crit} = 0.268(8)$. (b) The colloid cumulant $U_N(\eta_{\rm col})$ is plotted against the colloid packing fraction $\eta_{\rm col}$ at constant $\eta_{\rm pol}^{\rm crit} = 0.264$ The intersection is at $\eta_{\rm col}^{\rm crit} = 0.108(10)$, which corresponds nicely with the previously determined intersection point. The inset in both figures shows the vicinity of the intersection point magnified.

tracted from the simulation along the rectilinear diameter. The results can be seen in Figure 6. The cumulant intersection can be read off nicely and the crossing points agree within error margins. For the critical polymer packing fraction we find $\eta_{\rm crit}^{\rm pol} = 0.268(8)$, which is in nice agreement with the previously determined value of $\eta_{\rm extrapolated}^{\rm pol} = 0.264(10)$. The critical colloid packing fraction is determined independently as $\eta_{\rm crit}^{\rm col} = 0.108(10)$. The crossings from Figure 6(a) and (b) are consistent with each other, which can also be seen in Figure 5 since the error bars overlap. As expected, the critical polymer packing fraction has to be slightly adjusted compared to the cumulant intersection from the rectilinear diameter, while the critical colloid packing fraction agrees within the margin of error. As our best estimate for the critical point we choose the respective packing fractions obtained from the cumulant crossings at constant $\eta_{\rm pol}$ and $\eta_{\rm col}$ and thus obtain $\left(\eta_{\rm col}^{\rm crit} \middle/ \eta_{\rm pol}^{\rm crit}\right) = (0.108(10)/0.268(8))$. Note that the intersection of the cumulants are to some degree insensitive to minor variations of the other parameter as revealed by a comparison with the results from section III A.

D. Critical exponent β

With the knowledge of the critical point and the coexistence curve we can calculate the critical exponent β. The continuous Asakura-Oosawa model, which is used as a basis for the active model discussed here, belongs to the Ising universality class[36]. In three dimensions one would thus expect $\beta = 0.3269(6)$[59]. Close to the critical point the magnetization M scales in the Ising model as

$$M = M_0 \varepsilon^{\beta}, \tag{11}$$

with ε being the distance to the critical point. In the continuous Asakura-Oosawa model this corresponds to:

$$M = \sqrt{\left(\eta_{\rm col}^{\rm liquid} - \eta_{\rm col}^{\rm gas}\right)^2 + \left(\eta_{\rm pol}^{\rm liquid} - \eta_{\rm pol}^{\rm gas}\right)^2} \tag{12}$$

$$\varepsilon = \frac{\sqrt{\left(\frac{1}{2}\left(\eta_{\rm col}^{\rm liquid}+\eta_{\rm col}^{\rm gas}\right)-\eta_{\rm col}^{\rm crit}\right)^2+\left(\frac{1}{2}\left(\eta_{\rm pol}^{\rm liquid}+\eta_{\rm pol}^{\rm gas}\right)-\eta_{\rm pol}^{\rm crit}\right)^2}}{\sqrt{\left(\eta_{\rm col}^{\rm crit}\right)^2+\left(\eta_{\rm pol}^{\rm crit}\right)^2}} . \tag{13}$$

In Figure 7 the order parameter M, calculated from the

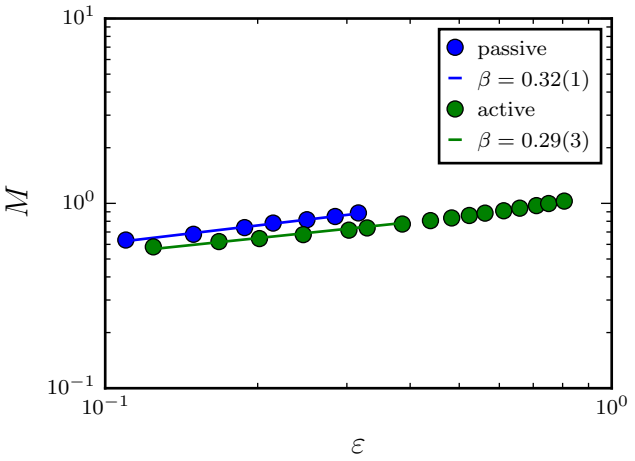

Figure 7. Comparison of the critical exponent β of the active and the passive model. The points are the respective values as extracted from the phase diagrams in Figure 2, while the line represents a fit from which the critical exponent β is determined. The error is calculated by repeating the fit for different critical points within the error bars.

phase diagrams in Figure 2, is plotted against ε which was determined with the respective critical points (for the passive case we use the literature value from[37]) in a log-log plot. For the passive case we recover the 3d-Ising value $\beta = 0.32(1)$ as expected. The active case has a value of $\beta = 0.29(3)$ and is thus close to the value of the 3d-Ising universality class as well. Even though the fit in Figure 7 matches the data points nicely, we have to assign a large uncertainty to the critical exponent for the active system. This is due to the error bars of the critical point, which in turn affects the estimation of ε (Eq. (13)). In order to account for that, we have calculated ε for various choices for the critical point (within the error bars) and repeated the fit. We then choose the error for β as the standard deviation of all possible choices. For bigger ε we get a deviation from the linear behavior on the log-log plot, and we thus do not account for them in the fit. The system, however, is only expected to follow this power law for small ε anyway. It should be noted that the model discussed here will be strongly influenced by the underlying passive model and thus one would expect to find a crossover region between Ising critical behavior and possibly a critical behavior corresponding to the universality class for active particles. Other models for active particles that introduce a phase separation instead of facilitating an already existing one might be better suited to study the question of universality.

E. Critical exponent ν

To determine the critical exponent ν we use the cumulant intersection of the polymers. The slope of the cumulants at the critical point can be extracted from Figure 6(a). It is expected that $\frac{dU_L}{d\eta_{\text{col}}}$ scales with L as[60]

$$\frac{dU_L}{d\eta_{\text{pol}}} \propto L^{\frac{1}{\nu}} \quad . \tag{14}$$

The slope at the critical point does not change rapidly, thus we determine it via a linear fit over the five state points that are closest to the critical polymer packing fraction. However, the slope in Figure 6(a) is negative, therefore we investigate the inverse cumulant Q_L and rewrite Eq. (14) to

$$\frac{dQ_L}{d\eta_{\text{pol}}} \propto L^{-\frac{1}{\nu}} \quad . \tag{15}$$

The critical exponent ν is then compared to the 3d-

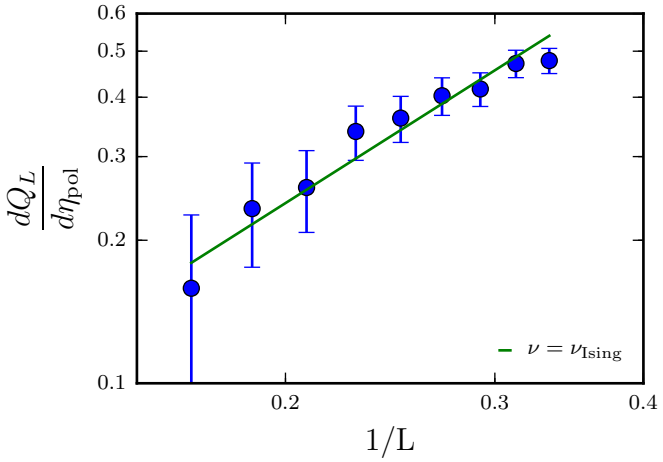

Figure 8. Comparison of the critical exponent ν from the slope of the cumulants from Figure 6(a) with ν_{Ising}[61]. All integer values between $N = 8$ and $N = 16$ are considered in this figure. Both axes have a logarithmic scale.

Ising value of $\nu_{\text{Ising}} = 0.63002(10)$[61] for all subboxes in the range of $N = 8 - 16$, which is shown in Figure 8. While we get consistent results with the Ising value of ν, the error bars of the subsystems are large and the data range is very limited due to the limited range of subbox sizes so that the scaling is observed on less than a decade. This causes a large uncertainty in a fit to the data points in Figure 8 with Eq. (15), which results in $\nu = 0.64(6)$. For still smaller systems a plateau is expected as one can no longer observe any fluctuations. For bigger systems correlations due to the finite size of the simulated box S influence the system and the statistical accuracy is decreased.

IV. DISCUSSION AND CONCLUSION

We have discussed a method of how to estimate the location of the critical point in a system of active particles analyzing the density fluctuations in subboxes.

The problem is difficult since one has to search in a two-dimensional space of densities $\left(\eta_{\mathrm{col},\eta_{\mathrm{pol}}}\right)$, and thus the critical point of our active system can only be determined with modest accuracy as $\eta_{\mathrm{crit}}^{\mathrm{col}} = 0.108(10)$ and $\eta_{\mathrm{crit}}^{\mathrm{pol}} = 0.268(8)$. Note that the subblock-density-distribution method we used is general and as such should apply to each density driven phase separation. The iterative approach that we have used to find the critical point is necessary since in this model the order parameter of the phase transition is an a priori unknown linear combination of both packing fractions. In a model with an intensive control parameter, e.g. the temperature in a Lennard-Jones system, or the active velocity in an active Brownian particle system, the search for the critical point is simpler.

The model used was chosen to feature a phase transition in the limit of no activity in order to have a critical point. While this model therefore is suitable to discuss the determination of the critical point it will be influenced by the underlying passive model. Our results for the critical exponents β and ν are consistent with the Ising universality class. For smaller values of f_A we expect the critical point to steadily shift towards the passive value. If the active system very close to its critical point exhibits critical behavior of a different universality class, further away from the critical point this is expected to be hidden by crossover effects. We can not rule out that this consideration is the correct interpretation of our findings.

ACKNOWLEDGEMENTS

We would like to thank S.K. Das, S. Egorov and M.P. Allen for fruitful discussions. BT acknowledges the Graduate School Materials Science in Mainz for partial financial support in form of a DFG-fellowship through the Excellence Initiative (GSC 266) as well as the SFB-TRR 146. BT, JS, TS and PV acknowledge support by the SPP1726 "Microswimmers" (grant number SP 1382/3-1 and VI 237/5-1). We thank the ZDV Mainz for computational resources.

REFERENCES

[1]M. Ballerini, N. Cabibbo, R. Candelier, A. Cavagna, E. Cisbani, I. Giardina, V. Lecomte, A. Orlandi, G. Parisi, A. Procaccini, *et al.*, Proceedings of the National Academy of Sciences **105**, 1232 (2008).

[2]Y. Katz, K. Tunstrøm, C. C. Ioannou, C. Huepe, and I. D. Couzin, Proceedings of the National Academy of Sciences **108**, 18720 (2011).

[3]V. Schaller, C. Weber, C. Semmrich, E. Frey, and A. R. Bausch, Nature **467**, 73 (2010).

[4]Y. Sumino, K. H. Nagai, Y. Shitaka, D. Tanaka, K. Yoshikawa, H. Chaté, and K. Oiwa, Nature **483**, 448 (2012).

[5]Sanchez Tim, Chen Daniel T. N., DeCamp Stephen J., Heymann Michael, and Dogic Zvonimir, Nature **491**, 431 (2012), 10.1038/nature11591.

[6]M. E. Cates, D. Marenduzzo, I. Pagonabarraga, and J. Tailleur, Proceedings of the National Academy of Sciences **107**, 11715 (2010).

[7]H. P. Zhang, A. Be'er, E.-L. Florin, and H. L. Swinney, Proceedings of the National Academy of Sciences **107**, 13626 (2010).

[8]Y. Yang, J. Elgeti, and G. Gompper, Physical review. E, Statistical, nonlinear, and soft matter physics **78**, 061903 (2008).

[9]R. Dreyfus, J. Baudry, M. L. Roper, M. Fermigier, H. A. Stone, and J. Bibette, Nature **437**, 862 (2005).

[10]V. Magdanz, S. Sanchez, and O. G. Schmidt, Advanced materials (Deerfield Beach, Fla.) **25**, 6581 (2013).

[11]H.-R. Jiang, N. Yoshinaga, and M. Sano, Phys. Rev. Lett. **105**, 268302 (2010).

[12]I. Buttinoni, G. Volpe, F. Kümmel, G. Volpe, and C. Bechinger, Journal of Physics: Condensed Matter **24**, 284129 (2012).

[13]J. R. Howse, R. A. L. Jones, A. J. Ryan, T. Gough, R. Vafabakhsh, and R. Golestanian, Phys. Rev. Lett. **99**, 048102 (2007).

[14]H. Ke, S. Ye, R. L. Carroll, and K. Showalter, J. Phys. Chem. A **114**, 5462 (2010).

[15]J. Palacci, C. Cottin-Bizonne, C. Ybert, and L. Bocquet, Phys. Rev. Lett. **105**, 088304 (2010).

[16]J. Palacci, S. Sacanna, A. P. Steinberg, D. J. Pine, and P. M. Chaikin, Science **339**, 936 (2013).

[17]Bricard Antoine, Caussin Jean-Baptiste, Desreumaux Nicolas, Dauchot Olivier, and Bartolo Denis, Nature **503**, 95 (2013).

[18]Yan Jing, Han Ming, Zhang Jie, Xu Cong, Luijten Erik, and Granick Steve, Nat Mater **15**, 1095 (2016).

[19]D. Grossman, I. S. Aranson, and E. B. Jacob, New Journal of Physics **10**, 023036 (2008).

[20]J. Bialké, T. Speck, and H. Löwen, Phys. Rev. Lett. **108**, 168301 (2012).

[21]F. D. C. Farrell, M. C. Marchetti, D. Marenduzzo, and J. Tailleur, Phys. Rev. Lett. **108**, 248101 (2012).

[22]S. K. Das, S. A. Egorov, B. Trefz, P. Virnau, and K. Binder, Physical Review Letters **112**, 198301 (2014).

[23]Julian Bialké and Thomas Speck and Hartmut Löwen, Journal of Non-Crystalline Solids **407**, 367 (2015).

[24]M. E. Cates and J. Tailleur, Annu. Rev. Condens. Matter Phys. **6**, 219 (2015).

[25]B. Trefz, S. K. Das, S. A. Egorov, P. Virnau, and K. Binder, The Journal of Chemical Physics **144**, 144902 (2016).

[26]G. S. Redner, M. F. Hagan, and A. Baskaran, Physical review letters **110**, 055701 (2013).

[27]J. Stenhammar, D. Marenduzzo, R. J. Allen, and M. E. Cates, **10**, 1489 (2014).

[28]A. Wysocki, R. G. Winkler, and G. Gompper, EPL (Europhysics Letters) **105**, 48004 (2014).

[29]V. Prymidis, H. Sielcken, and L. Filion, Soft Matter **11**, 4158 (2015).
[30]J. Schwarz-Linek, C. Valeriani, A. Cacciuto, M. E. Cates, D. Marenduzzo, A. N. Morozov, and W. C. K. Poon, Proceedings of the National Academy of Sciences **109**, 4052 (2012).
[31]J. Stenhammar, R. Wittkowski, D. Marenduzzo, and M. E. Cates, Physical review letters **114**, 018301 (2015).
[32]A. Y. Grosberg and J.-F. Joanny, , 5 (2015), arXiv:1502.08034.
[33]S. Asakura and F. Oosawa, The Journal of Chemical Physics **22**, 1255 (1954).
[34]S. Asakura and F. Oosawa, Journal of polymer science **33**, 183 (1958).
[35]A. Vrij, Pure and Applied Chemistry **48**, 471 (1976).
[36]R. Vink, J. Horbach, and K. Binder, Physical Review E **71**, 011401 (2005).
[37]J. Zausch, P. Virnau, K. Binder, J. Horbach, and R. L. Vink, Journal of Chemical Physics **130**, 64906 (2009).
[38]K. Binder, P. Virnau, and A. Statt, The Journal of chemical physics **141**, 140901 (2014).
[39]D. Winter, P. Virnau, J. Horbach, and K. Binder, EPL (Europhysics Letters) **91**, 60002 (2010).
[40]A. Hucht, Physical review. E, Statistical, nonlinear, and soft matter physics **80**, 061138 (2009).
[41]T. Vicsek, A. Czirók, E. Ben-Jacob, I. Cohen, and O. Shochet, Phys. Rev. Lett. **75**, 1226 (1995).
[42]A. Czirók, H. E. Stanley, and T. Vicsek, Journal of Physics A: Mathematical and General **30**, 1375 (1997).
[43]G. Grégoire and H. Chaté, Phys. Rev. Lett. **92**, 025702 (2004).
[44]M. Nagy, I. Daruka, and T. Vicsek, **373**, 445 (2007).
[45]M. Aldana, V. Dossetti, C. Huepe, V. M. Kenkre, and H. Larralde, Phys. Rev. Lett. **98**, 095702 (2007).
[46]V. Prymidis, S. Paliwal, M. Dijkstra, and L. Filion, , 8 (2016), arXiv:1606.06585.
[47]A. P. Solon and J. Tailleur, Phys. Rev. E **92**, 042119 (2015).
[48]J. A. Barker and D. Henderson, The Journal of Chemical Physics **47**, 4714 (1967).
[49]G. S. Grest and K. Kremer, Physical Review A **33**, 3628 (1986).
[50]D. Frenkel and B. Smit, *Understanding molecular simulation: from algorithms to applications*, Vol. 1 (Academic press, 2001).
[51]K. Binder, Zeitschrift für Physik B Condensed Matter **43**, 119 (1981).
[52]M. Rovere, D. W. Hermann, and K. Binder, Europhysics Letters (EPL) **6**, 585 (2007).
[53]M. Rovere, P. Nielaba, and K. Binder, Zeitschrift für Physik B Condensed Matter **90**, 215 (1993).
[54]H. Watanabe, N. Ito, and C. K. Hu, Journal of Chemical Physics **136**, 204102 (2012).
[55]J. Rowlinson and F. Swinton, *Liquids and Liquid Mixtures* (Butterworth, 1982).
[56]J. V. Sengers, *Phase transitions: Cargèse 1980* (Plenum Publishing Corporation, 1982) Chap. Universality of critical phenomena in classical fluids, p. 95.
[57]Y. C. Kim, M. E. Fisher, and G. Orkoulas, Physical review. E, Statistical, nonlinear, and soft matter physics **67**, 061506 (2003).
[58]Y. C. Kim, M. E. Fisher, and E. Luijten, Physical Review Letters **91**, 065701 (2003), 0304032.
[59]A. L. Talapov and H. W. J. Blöte, Journal of Physics A: Mathematical and General **29**, 5727 (1996).
[60]R. L. C. Vink, K. Binder, and J. Horbach, Physical Review E - Statistical, Nonlinear, and Soft Matter Physics **73**, 56118 (2006).
[61]M. Hasenbusch, Phys. Rev. B **82**, 174433 (2010).